Revealing new hydrocarbon potential through *Q*-compensated prestack depth imaging at Wenchang Field, South China Sea

Lin Li[1], Lie Li[1], Tao Xu[1], Min Ouyang[1], Yonghao Gai[1], Yitao Chen[2], Xiaodong Wu[2], Yongxia Liu[3], and Jason Sun[2]

https://doi.org/10.1190/tle38080604.1.

Abstract

Wenchang Field in the South China Sea contains a well-developed fault system, resulting in complex subsurface geology. Imaging the complex fault system plays an important role in hydrocarbon exploration in this area since the fault system forms a link between the source rocks and reservoirs. However, it is difficult to obtain a high-quality depth image of the fault system due to the effects of complex velocity and seismic absorption. Inaccurate depth velocities lead to fault shadows and structure distortions at the target zone. Absorption effects further deteriorate seismic imaging as they cause amplitude attenuation, phase distortion, and resolution reduction. We demonstrate how a combination of high-resolution depth velocity modeling and *Q* imaging work together to resolve these challenges. This workflow provides a step change in image quality of the complex fault system and targeted source rocks at Wenchang Field, significantly enhancing structure interpretation and reservoir delineation. A couple of commercial discoveries have been made, and several other potential hydrocarbon reservoirs have been identified based on the reprocessed data, which reveal new hydrocarbon potential in this region.

Introduction

Wenchang Field, situated in the Pearl River Mouth Basin in the northern part of the South China Sea, is an area of active hydrocarbon exploration and production (Figure 1a). The Pearl River Mouth Basin is a continent-marginal and extensional basin that developed Wenchang continental faulted sedimentation in the rifting stage of the Paleogene period. In Wenchang Field, the middle-deep lacustrine source rocks consist of taupe mud and shale, which contain abundant C30 4-methyl steranes (Chen and Cunmin, 1993). These types of source rocks are of high quality, as they were deposited in a lacustrine-weak oxidation-weak reduction sedimentary environment (Jiang et al., 2015). These source rocks bearing oil-generating potential are characterized by abnormally high amplitudes and dominant low frequency on the seismic image, and they have been validated by recent drilling in the Wenchang 19 Depression. Therefore, it has been hypothesized that high-quality middle-deep lacustrine source rocks are also present at the junction of Wenchang 14 and 19 depressions (Figure 1b), which, if validated, would significantly increase the exploration potential of Wenchang Field.

Above the deep source rocks lies a complex intraformational fault system, the Flower Fault System, which developed in the postrifting stage. There are many favorable traps with high exploration potential in the area. However, complex velocities, strong multiples, and low signal-to-noise ratio (S/N) in the target zone have compromised imaging quality. Figure 2a shows a typical section from legacy prestack depth migration (PSDM) processing located at the junction of Wenchang 14 and 19 depressions. Two important questions have persisted for years without receiving

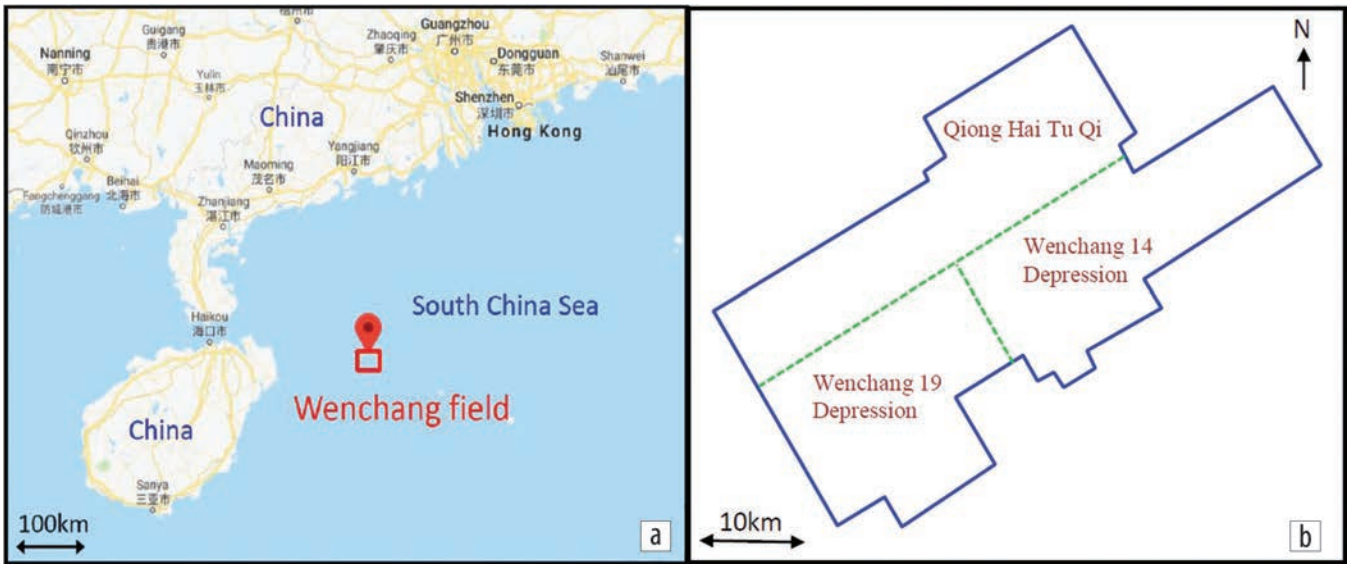

Figure 1. (a) Wenchang Field location. (b) Survey map of Wenchang 14 and 19 depressions and the Qiong Hai Tu Qi Survey in Wenchang Field.

[1]CNOOC, Zhanjiang, Guangdong, China. E-mail: lil@cnooc.com.cn; lilie@cnooc.com.cn; xutao3@cnooc.com.cn; ouyangm@cnooc.com.cn; gaiyh1@cnooc.com.cn.
[2]CGG, Singapore. E-mail: yitao.chen@cgg.com; xiaodong.wu@cgg.com.cn; jason.sun@cgg.com.
[3]CGG, Beijing, China. E-mail: yongxia.liu@cgg.com.

proper answers. Are source rocks properly positioned in this area? Where is the Zhu III South Fault (also called the Big South Fault)? Conflicting events, strong migration swings, and residual multiples seriously affect structure imaging in the legacy data. This poses a huge exploration risk and prevents a good new understanding of petroleum systems in the area. The data have been reprocessed and reinterpreted multiple times without resolving uncertainty in the reservoir areas.

To improve the seismic image, reprocessing of Wenchang 14 and 19 depressions and the Qiong Hai Tu Qi Survey (Figure 1b) in Wenchang Field was performed using high-resolution depth velocity modeling and *Q*-compensated prestack depth migration (QPSDM). Combined with broadband processing technology and a comprehensive demultiple package, reprocessing significantly improved fault imaging, source rock delineation, and data S/N. As a result, as shown in Figure 2b, the two questions have been much better answered. In the legacy image, the deep source rocks are poorly focused, and they extend into the basement below the Big South Fault. The Big South Fault is hardly visible and is crosscut by migration swings. In the new QPSDM image, the question of where the Big South Fault sits has been better answered with a much clearer fault plane. The image provides critical information for understanding how hydrocarbons migrated from source rocks and were trapped.

We will introduce how high-resolution depth velocity modeling and QPSDM imaging work together to provide the uplift seen on the seismic data. The improved imaging quality enables a fresh structural interpretation of this area, helping to identify a number of new reservoirs and greatly enhancing exploration potential.

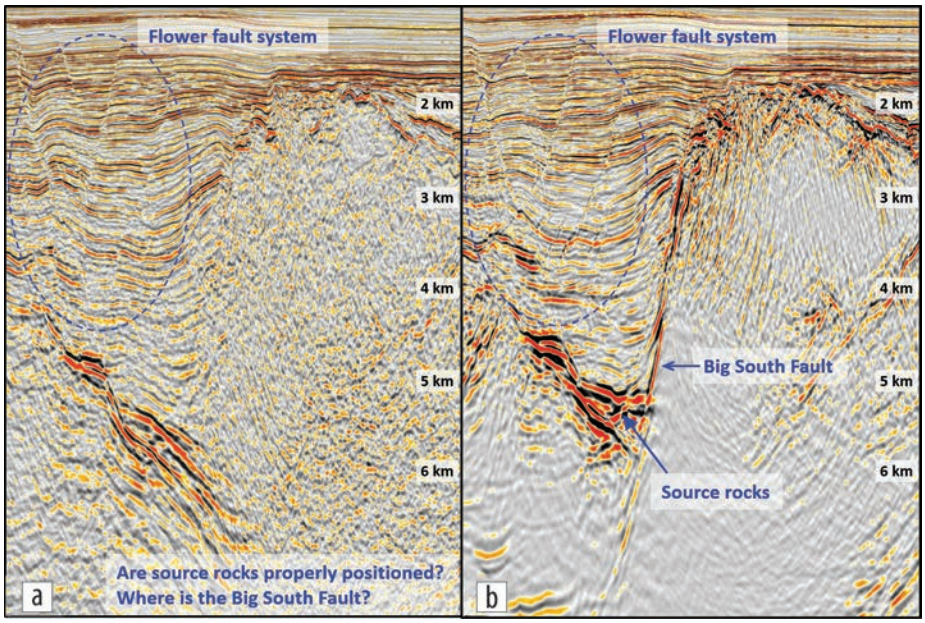

Figure 2. (a) Legacy PSDM image. The Big South Fault is hardly visible and the middle-deep lacustrine source rocks are poorly imaged, which affects interpretation of the middle-deep lacustrine source rocks and their possible link to reservoirs. (b) New QPSDM image with improved imaging of the fault system and source rocks.

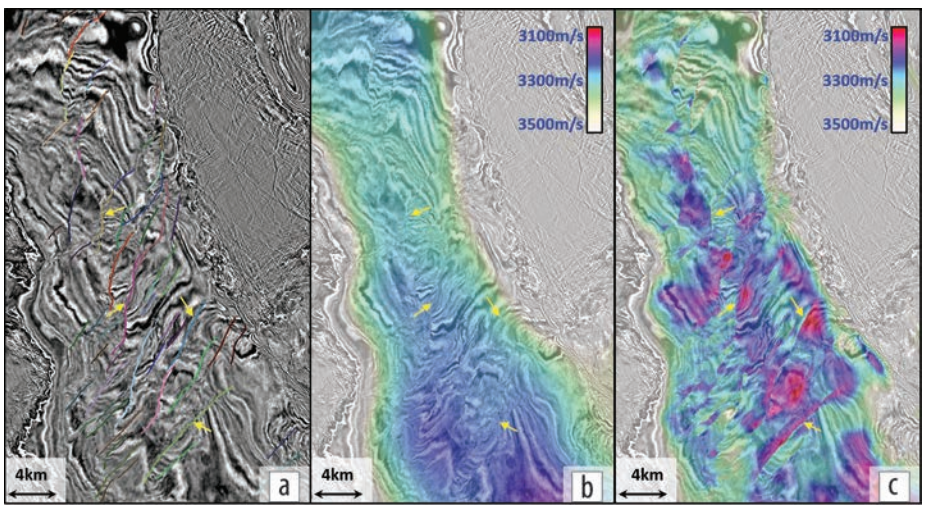

Figure 3. Seismic depth slice at 2400 m. (a) Fault system distribution in Wenchang Field. (b) Initial velocity model. (c) Final velocity model. Depth model building successfully restored the velocity contrast crossing the fault planes and produced a high-resolution depth velocity model.

High-resolution depth velocity modeling

The complex fault system is well developed in Wenchang Field, and the complexity of its velocity poses serious challenges for imaging the faulted structures and underlying source rocks. To overcome these challenges, high-resolution tomography was applied for depth velocity model building.

We started the velocity model building process with nonlinear multilayer tomography (Guillaume et al., 2013). High-quality residual moveout picking is essential for high-resolution tomography to ensure velocity inversion stability and convergence. An automatic picking scheme was used to pick the residual curvature on the common image gathers (CIGs) and the reflector dipping information on the stack. Picking density was high in x, y, and z directions to ensure a more stable update. In this study, the CIG grid was 50 × 50 m, and the minimum event separation along the z direction was 20 m. As a key component of high-resolution depth velocity modeling, fault-constrained tomography (Birdus, 2007; Guo et al., 2015) was used to restore the velocity variation across faults. The fault planes were interpreted from seismic images and supplied to tomography engines with residual moveout picks (Figure 3a). High-resolution 3D tomography used fault planes as part of the constraint during the velocity update. The internal tomographic regularization was also modified to honor and restore velocity

contrast across the faults. The velocity update was not limited to just near fault planes but was also applied to complete tomographic layers.

Figures 3b and 3c show the initial velocity model and final velocity model, respectively, overlaid on a seismic depth slice. The velocity color map for these displays was designed to highlight horizontal velocity variation across faults. The depth velocity modeling workflow successfully restored velocity contrasts and built a high-resolution velocity model over the complex fault system. Figure 4 shows the velocity and corresponding PSDM stacks across the fault system with the initial and final depth velocity models. High-resolution depth velocity modeling effectively resolved the fault shadows so that structural distortions were mitigated and event continuity was improved.

Imaging of middle-deep lacustrine source rocks is essential for a full understanding of hydrocarbon potential. Velocity errors in the fault system will not only lead to fault shadow issues but will also accumulate in the deeper sections and distort source rock images. Figure 5a shows the PSDM stack at the source rock zone with the initial velocity model. The PSDM image shows the nongeologic conflicting structures where the deep-dipping fault cuts through source rock events. This distortion is caused by the velocity error in the shallow Flower Fault System. After restoring the velocity details, the source rock events converged to the left side of the deep fault, and the PSDM image showed better geologic rationality in the target zone (Figure 5b). Figure 6a shows the PSDM stack overlaid with the final depth velocity model. The final velocity model followed the seismic structures well and restored the sharp velocity contrast crossing the fault plane. This was key to obtaining a clear image of the targeted source rocks. Figure 6b shows three PSDM CIGs in the target zone. The events in CIG are flat in the shallow Flower Fault System and deep source rock structures, which confirms accuracy of the depth velocity model.

Q-compensated prestack depth migration

Absorption of seismic waves causes amplitude attenuation, wavelet phase distortion, and seismic resolution reduction at deeper targets. Steeply dipping faults will be more affected as the rays travel farther than those of flat events, which leads to a larger absorption effect. Figures 7a and 7b show the ray-tracing analysis of the Big South Fault and a flat event at the same depth of 3.5 km, respectively. The traveltime of wave propagation for the Big South Fault is approximately 4.4 s, which is nearly double that of the flat reflector. *Q* compensation as part of depth imaging is important to address the transmission loss and further improve the image quality of steeply dipping faults at Wenchang Field. In 3D QPSDM, an antidissipation filter as a function of velocity field and *Q* quality factor is integrated to form the *Q* migration operator, honoring the actual raypaths for imaging with compensation for both amplitude attenuation and phase distortion (Xie et al., 2009).

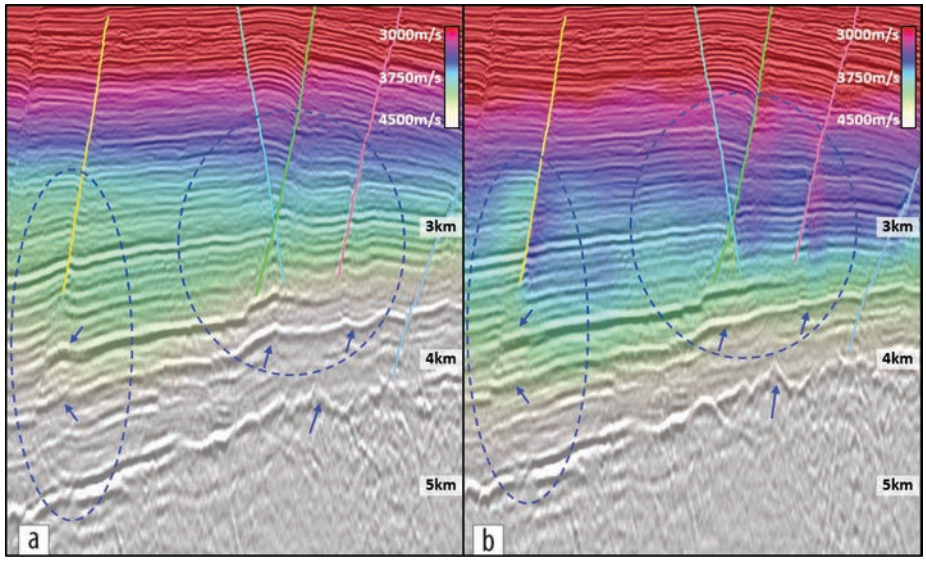

Figure 4. Velocity model and corresponding PSDM stacks across the fault system. (a) Initial depth velocity model and (b) final depth velocity model. High-resolution modeling resolved fault shadows and structural distortions and improved event continuity in and below the faulting zone.

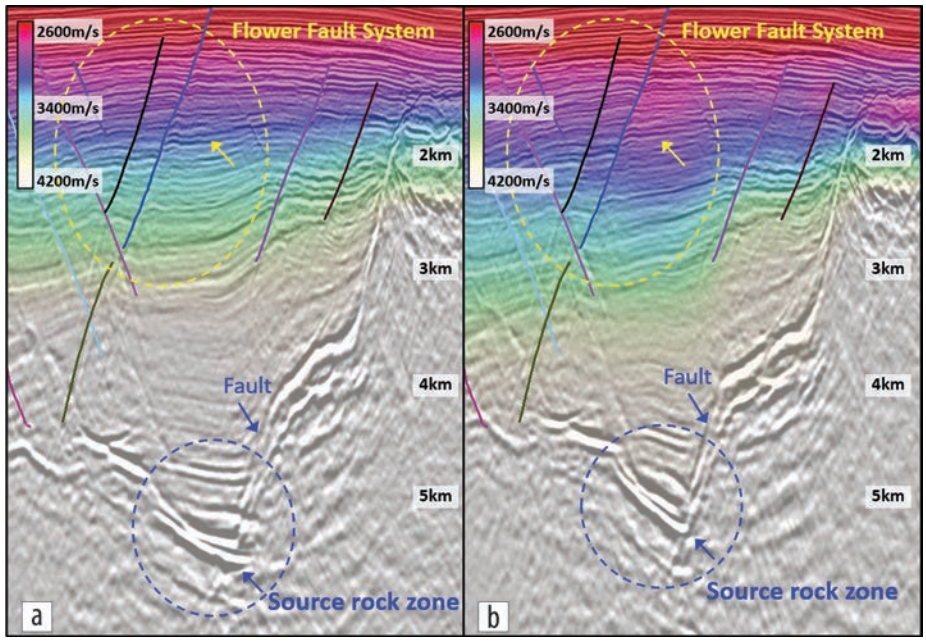

Figure 5. Velocity and corresponding PSDM stacks across the fault system and source rock zone. (a) Initial depth model. (b) Final depth model. High-resolution model building resolved structural distortions in the source rock zone.

There is no presence of absorption (Q) anomalies in the data, so a constant background Q quality factor of 150 using the spectral ratio method was derived and used for QPSDM. It is worth mentioning that another technology for absorption inversion called "volumetric Q tomography" (Gamar-Sadat et al., 2015) was tested on a small swath. The test result showed that there is no significant spatial variation in the Q model for this data, and both models were able to produce similar QPSDM images. As a comparison, conventional PSDM stack using the same depth velocity model has been carried out followed by 1D Q compensation. The 1D Q compensation does not honor true ray tracing, leading to inaccurate Q compensation for dipping structures. Figures 7c and 7d show a comparison of the PSDM image with 1D poststack Q compensation versus the QPSDM image. The QPSDM image successfully improved the imaging quality of steeply dipping reflectors.

Fault system interpretation and reservoir delineation

In the study area, the peak time of hydrocarbon generation was accompanied by active extensional tectonic movements in which the Big South Fault was formed. A good understanding of the fault provides important information about how hydrocarbons formed from source rocks, migrated, and were trapped, which is key to reservoir interpretation. Figure 8 shows a comparison of old and new geologic interpretations of the Big South Fault and basement overlaid on seismic. In the legacy data, the strong reflector beside the Big South Fault around a two-way traveltime (TWT) of 2 s (indicated by the blue dashed line) was interpreted as a basement boundary. As a result, the Big South Fault was interpreted more toward the northwest, as indicated by the black dashed line. The new QPSDM image revealed a well-stratified deep structure near the source rocks around a TWT of 3 s, which completely changes interpretation of the Big South Fault and the basement boundary, as shown in Figure 8b. This new result delivers a better understanding of the spatial relationship between the source rocks, basement, and the Big South Fault. With this improved understanding, a new reservoir structure with high potential has been identified near the newly interpreted Big South Fault.

Data reprocessing also helped reinterpretation of the Flower Fault System. Figure 9 shows a comparison of the Flower Fault interpretation based on legacy and new images. The previous interpretation result, based on legacy images, is a "shovel-type" Flower Fault System. Based on the current QPSDM images, the faulting structures were reinterpreted as a "seat-type" Flower Fault System. Considering the effect of tectonic inversion on fault deformation,

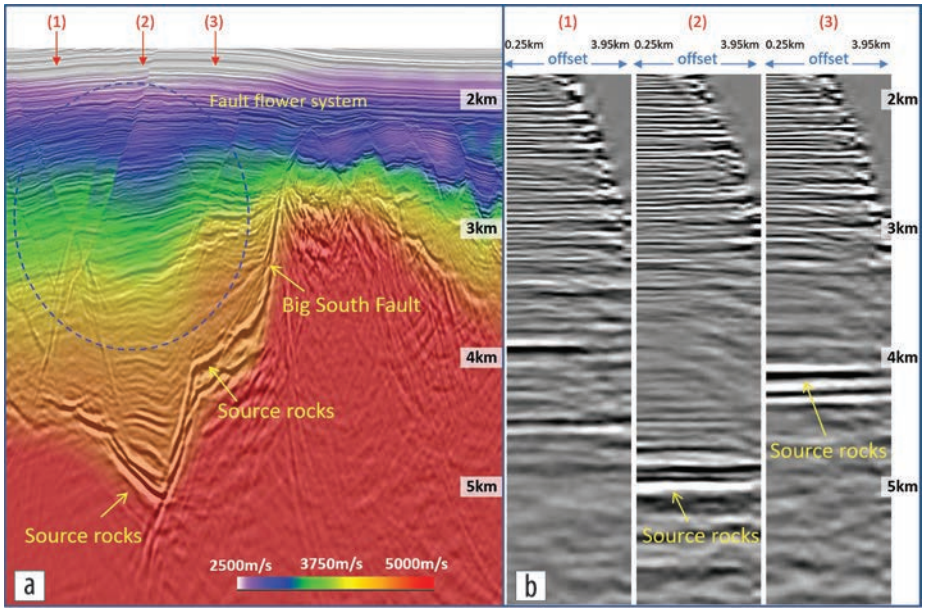

Figure 6. (a) PSDM stack overlaid with final depth velocity model. (b) PSDM CIG in the target zone.

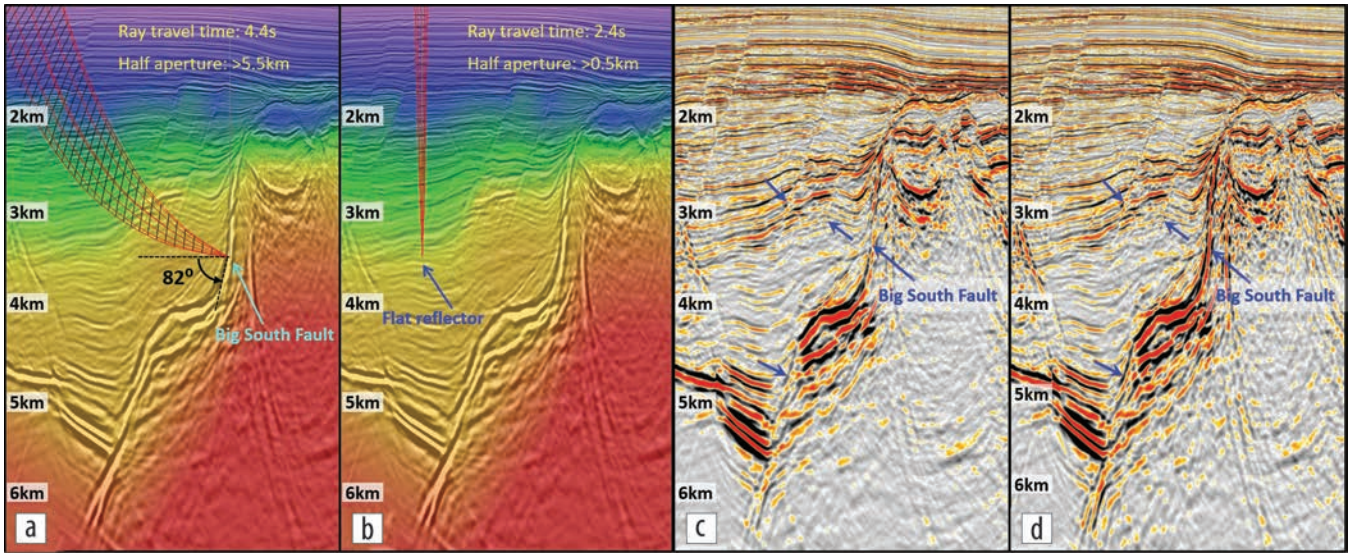

Figure 7. Ray tracing analysis of (a) a steeply dipping fault and (b) a flat event at the same depth. (c) PSDM image with 1D poststack Q compensation. (d) QPSDM image.

the new interpretation is more consistent with typical extension and dextral strike-slip deformation characteristics in this area. Based on the new interpretation, the Wenchang 19-10 reservoir structure was found and validated by recent drilling.

The new QPSDM result improved the image quality of deep source rocks and provided a more accurate delineation of the source rock zone. Figure 10a shows the source rock distribution in the Wenchang area. Based on the legacy images, 65 km^2 of the source rock zone was interpreted in this area. The new interpretation helps identify an additional 45 km^2 of the middle-deep lacustrine source rock zone. Extension of the interpreted source rock area greatly improves our insight into hydrocarbon exploration potential in Wenchang Field. With a better-imaged fault system and source rocks from the new data, target reservoirs have been reevaluated and reinterpreted as shown in Figure 10b. The dark and light green areas are commercial reservoirs and oil-bearing structures, respectively, which have been validated by recent drilling. Another seven potential hydrocarbon reservoirs (yellow areas in Figure 10b) have been identified.

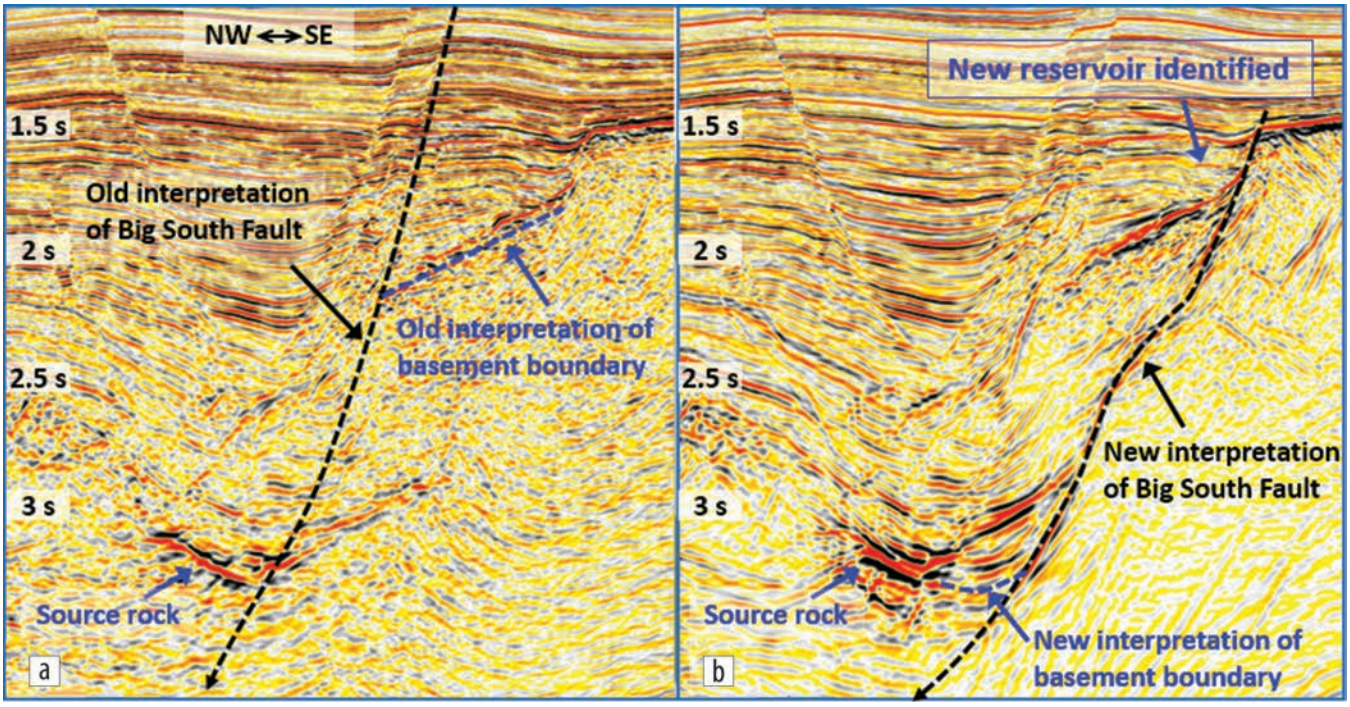

Figure 8. Interpretation of the Big South Fault and basement on (a) the legacy image and (b) the new QPSDM image in the time domain. The new result changes interpretation of the basement and Big South Fault and helps identify the new reservoir near the fault.

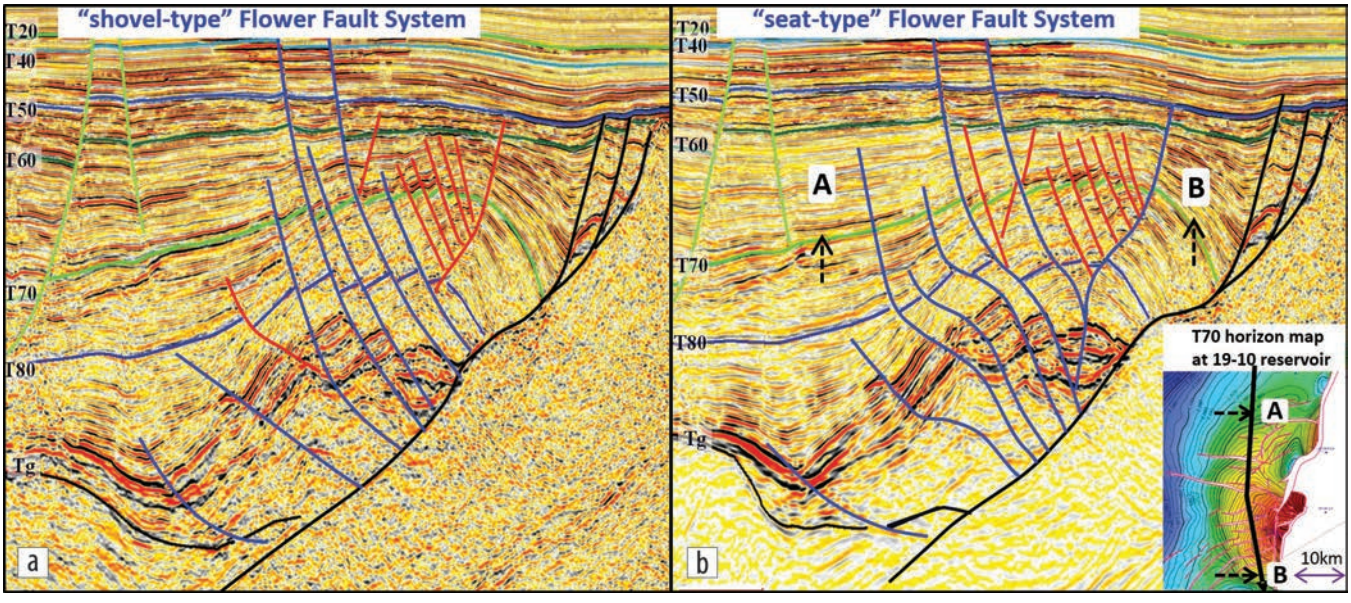

Figure 9. Flower Fault System interpretation based on (a) the legacy image and (b) the new QPSDM image in the time domain. The Flower Fault System changed from "shovel" to "seat" type. Reinterpretation played a role in the discovery of the Wenchang 19-10 reservoir.

Conclusions

The geologic complexities of Wenchang Field, Pearl River Mouth Basin, have historically impacted the quality of seismic imaging, which has been a major barrier for reducing exploration risk. We demonstrated successful application of a high-resolution depth velocity modeling and QPSDM imaging workflow to this data, which provides an effective solution for better imaging of the complex fault system. High-resolution depth velocity modeling successfully restored velocity contrasts in a complex fault system. With that, QPSDM resolved the geologic complexities with a clearer Flower Fault System and deep source rock imaging. The step change in imaging quality supplied key information for fault system interpretation, source rock mapping, and reservoir delineation. With better understanding of the petroleum system in Wenchang Field to support better well-placement decisions and more-effective field development, hydrocarbon exploration potential has been significantly enhanced.

To further improve imaging in this area, narrow-azimuth illumination is a major limitation. The illumination of faults is particularly sensitive to their orientation relative to acquisition direction. Wide-azimuth acquisition and imaging will further improve imaging quality of fault systems and could be a good investment considering the rich hydrocarbon potential of Wenchang Field. TLE

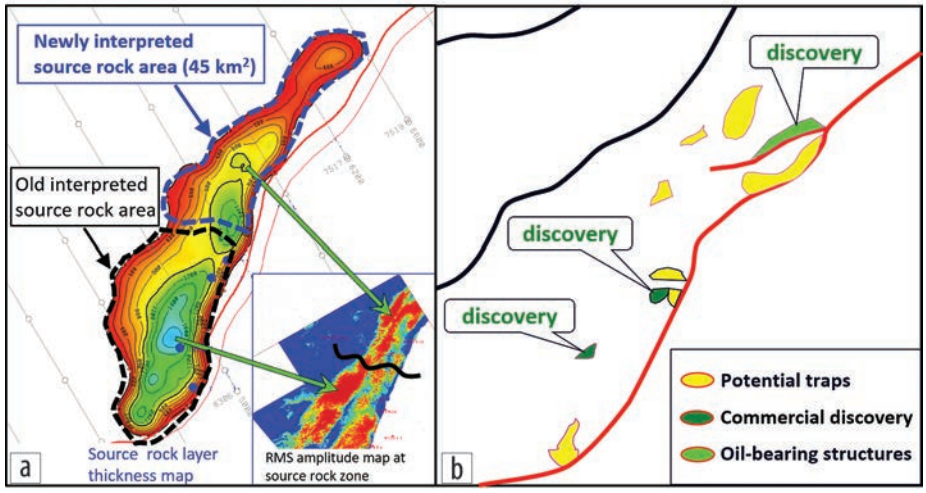

Figure 10. (a) Source rock distribution in the Wenchang area. (b) Interpreted target reservoir map based on the new QPSDM image. The dark and light green areas are commercial reservoirs and oil-bearing structures, respectively. The yellow areas are seven potential hydrocarbon reservoirs.

Acknowledgments

The authors thank CNOOC and CGG for permission to present the data and publish this work. They also thank Xiao-gui Miao and all colleagues who contributed to this work.

Data and materials availability

Data associated with this research are confidential and cannot be released.

Corresponding author: yitao.chen@cgg.com

References

Birdus, S., 2007, Removing fault shadow distortions by fault-constrained tomography: 77th Annual International Meeting, SEG, Expanded Abstracts, 3039–3043, https://doi.org/10.1190/1.2793102.

Chen, S., and P. Cunmin, 1993, Geology and geochemistry of source rocks of the Eastern Pearl River Mouth Basin, South China Sea: Journal of Southeast Asian Earth Sciences, **8**, no. 1–4, 393–406, https://doi.org/10.1016/0743-9547(93)90041-M.

Gamar-Sadat, F., P. Guillaume, A. Pica, G. Pignot, P. Poggi, A. Henry-Baudot, A. Prescott, A. Gacha, D. Carotti, and V. Prieux, 2015, Automatic gas pockets detection by high-resolution volumetric Q-tomography using accurate frequency peak estimation: 77th Conference and Exhibition, EAGE, Extended Abstracts, Th N107 10.

Guillaume, P., X. Zhang, A. Prescott, G. Lambaré, M. Reinier, J. Montel, and A. Cavalié, 2013, Multi-layer non-linear slope tomography: 75th Conference and Exhibition, EAGE, Extended Abstracts, Th 04 01.

Guo, Y., M. Fujimoto, S. Wu, and Y. Sasaki, 2015, Fault shadow removal over Timor Trough using broadband seismic, FWI and fault constrained tomography: 77th Conference and Exhibition, EAGE, Extended Abstracts, https://doi.org/10.3997/2214-4609.201412729.

Jiang, H., X. Pang, H. Shi, Q. Yu, Z. Cao, R. Yu, D. Chen, Z. Long, and F. Jiang, 2015, Source rock characteristics and hydrocarbon expulsion potential of the Middle Eocene Wenchang Formation in the Huizhou Depression, Pearl River Mouth Basin, South China Sea: Marine and Petroleum Geology, **67**, 635–652, https://doi.org/10.1016/j.marpetgeo.2015.06.010.

Xie, Y., K. Xin, J. Sun, C. Notfors, A. K. Biswal, and M. K. Balasubramaniam, 2009, 3D prestack depth migration with compensation for frequency dependent absorption and dispersion: 79th Annual International Meeting, SEG, Expanded Abstracts, 2919–2923, https://doi.org/10.1190/1.3255457.